A Case Study on Waveguide Fed Broad Wall Two Elements Longitudinal Slot Array Antenna for Design of Gain

[1]Hare Ram Jha*, [2]Manish Korde, [3]Deepesh Kumar Shrivas, [4]Rahul Nigam and [5]Kamini Vishwakarma

[1, 2, 4]Department of Electronics Engineering,
[3,5]Department of Computer Science & Engineering,
Medicaps University, Indore
Indore-453331, Madhya Pradesh, India

***Abstract*- This work aimed to build and analyze eight different configurations of waveguide fed broad wall two element longitudinal slot array antennas for high-frequency X-band applications (8.2-12.4 GHz). Modern wireless communication systems are well-suited to these antennas due to their low loss, structural simplicity, and high gain. A conventional WR-90 waveguide is milled on one or both faces of the waveguide to create two-port, two-element series, or shunt slot array structures, and the designs incorporate a variety of combinations of similar and unique slot lengths. The electromagnetic behavior was assessed for each configuration by computing the reflection coefficient ($|S_{11}|$) and transmission coefficient ($|S_{21}|$) using MATLAB versions of the Multiple Cavity Modelling Technique (MCMT). The findings were confirmed by the use of Ansoft HFSS full-wave simulations. The correctness and computational efficiency of the MCMT approach were confirmed by the close agreement that was found across all cases when comparing MCMT and HFSS data. Case VI performed the best of the eight configurations, with wide impedance matching, high transmission, and constant strong gain. These results prove that MCMT is a trustworthy forecasting technique for high-frequency antenna models and show how effective optimized slot is designed. In order to validate and design efficient slot array antennas for use in wireless communication systems, radar, and satellites, the study offers a thorough evaluation methodology.**

***Index Terms*- Array, antenna design, longitudinal slot, multiple cavity modelling technique, Waveguide.**

I. INTRODUCTION

Longitudinal slot array antennas supplied by waveguides are preferred in high-frequency communication systems due to their reliability. Due to their numerous advantageous characteristics, such as their high efficiency, capacity to accurately manage the aperture distribution, high gain, and ability to handle high power levels, waveguide slot array antennas (WSAAs) find extensive application in radar systems and satellite communications [1]. Ensure their continued utility in the modern day, even as wireless communications and information technologies advance. These characteristics make waveguide-fed large wall longitudinal slot array antennas ideal for uses requiring simple, effective high-frequency transmission [2-3]. Slot antennas provide a number of benefits over other kinds of antennas, including being easy to install, durable, inexpensive, and simple. High data transfer rates are necessary in modern communication systems, but attenuation during propagation is another obstacle. Solutions to mitigate propagation attenuation in high-gain antennas. These antennas enhance the communication range and signal strength by directing the radiated energy in a specified direction. Another well-known option is the slot array antenna, which makes use of many slots to boost directivity, gain, and overall efficiency while compensating for propagation losses. Improving gain and directivity relies heavily on the optimal design of slot array antennas [4-6].
A longitudinal slot antenna that was supplied by waveguide was initially found by George C. Southworth in 1936. In this area, Watson, Stevenson, and Booker made groundbreaking contributions. After conducting experiments to determine the electric field of the slot aperture, Stevenson offered theoretical ideas that Watson used in his formulation. In order to prove that dipoles and slots are similar, Booker used waveguide Green's functions and Babinet's principle [7-9] to solve the integral equation. This research was also aided by silver [10]. A huge array of antennas using a periodic construction method was introduced by Edelberg and Oliner in 1960. In which a two-dimensional array of slots was utilized, with a distinct waveguide feeding each slot [11]. The study of the mutual impedance of two adjacent slots was published in an article by Das and Sanyal in 1971 [12]. The resonant length against slot offset for certain waveguide dimensions was given

by Elliot and Stern in 1985, and frequency is computed using the method of moments [13]. The study of a rectangular waveguide with a large wall inclined slot was presented by Rengarajan [14] in 1990. B. Duan et al. [15] demonstrated the functionality of surface-distorted planar slotted waveguide arrays in 2011. When it comes to high-gain broadband waveguide broad-wall longitudinal slot array antennas, Gayen and Das [16] presented a moments-based analysis approach in 2013. For waveguide-milled series and shunt slot array antennas with matching or different electrical lengths, Jha and Singh [17] investigated two longitudinal slots in 2015. Building the two-element series and the shunt slot array separately is the first step. Two longitudinal slots with matching or different electrical lengths that are milled on one or both sides of a waveguide for a shunt slot array antenna are also studied by Jha and Singh in 2016 [18]. Subsequently, Jha and Singh [19] designed a slot doublet antenna in 2017.

No author in the literature review stated earlier investigated the simultaneous behavior of scattering parameters and gain characteristics in a two-port, two-element series and shunt slot array antenna, with the exception of Jha and Singh. While Jha and Singh do address one case study—the design of a shunt slot array antenna—they leave the scope of the combined case study open. Several designs and evaluations of shunt and series slot array antennas are presented in this enhanced case study.

This article takes a look at the scattering parameter that results from the mutual impedance between two milling slots on either the top or bottom side of the conventional waveguide's broad wall (WR-90) that have the same or differing electrical lengths. Fig. 1 shows that a grand total of eight different configurations are generated. Next, create the whole thing and test the antenna's gains and scattering settings with Ansoft's High Frequency Simulation Structure (HFSS). Slots are primarily defined by two properties: the electrical length and the offset from the centre. While the offset determines the power emitted from the slot into the half space, the electrical length of the slot often defines its resonant frequency. Radiating slots with varied electrical lengths (which correlate to varying resonance frequencies) make up the array. Because of some inherent quality, each of them will have its own distinct resonance frequency.

A. Theory of Design

Figure 1 shows that a grand total of eight different configurations are generated. Each of the eight distinct standard waveguides (WR-90) has two slots cut into it, as seen in Fig. 1. The calculation for the offset position and slot length is as follows: [3]. Fig. 1 (a) and Fig.1 (c) show two-port, two-element shunt slot array antennas with identical and different electrical slot lengths, respectively, and slots are milled on both waveguide faces. Fig. 1(b) and Fig. 1(d) show two-port, two-element shunt slot array antennas with identical and different electrical slot lengths, respectively, in contrast to waveguides with slots milled on just one face. Fig. 1(d) and Fig. 1(f) demonstrate two-port, two-element shunt slot array antennas with identical and different electrical slot lengths machined on the two waveguide faces, respectively. The two-port, two-element shunt slot array antennas in Fig. 1(e) and Fig. 1(g) have electrical slot lengths that are different from one another, in contrast to the waveguides in the former. The exact measurements of the WR-90 waveguide, including its overall length, width, spacing, right/left plate to slot centre distance, and slot offset location, can be found in Table 1. The width of the waveguide is 10.16 mm, and the length of the narrow wall is 22.86 mm.

Fig. 1 can be used to make eight examples here. Fig. 1(a) is regarded as case I. Fig. 1(b) as case- II, Fig. 1(c) as case III, Figure 1(d) as case IV, Fig. 1 (e) as case-V, Fig. 1(f) as case-VI, Figure 1(g) as case-VII, and Fig. 1(h) as case-VIII.

The eight distinct configuration case structures listed above are designed in accordance with Fig. 1, with Table:1 accounting for specifications. In the Ansoft High Frequency Simulation Structure (HFSS) environment, both ports are activated independently in cases I, II, III, IV, V, VI, VII, and VIII. Fig. 2 displays three-dimensional images with electric fields for various scenarios.

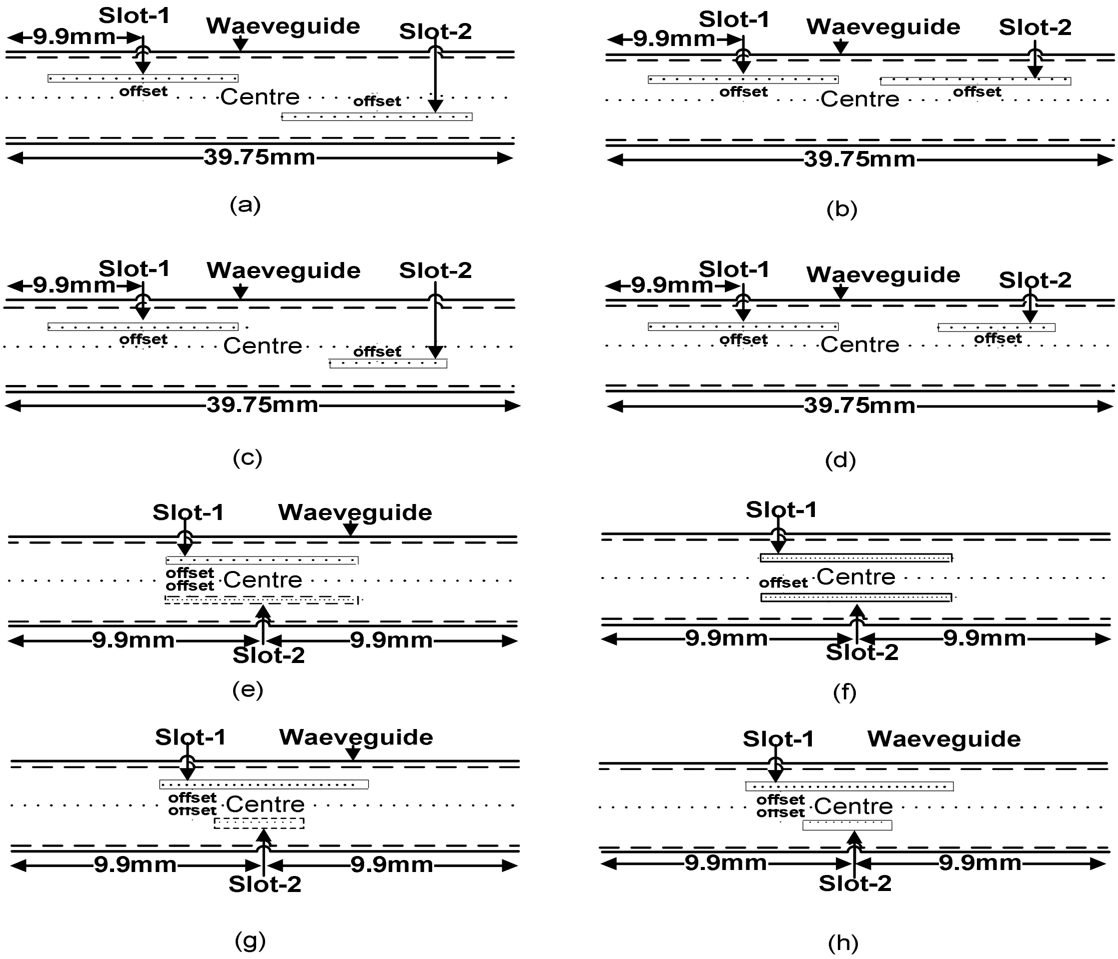

Fig.1. Two dimensional view of (a) case-I (b) case-II, (c) case-III (d) case-IV, (e) case-V, (f) case-VI, (g) case-VII, and (h) case-VIII.

Table 1: Dimension of various configuration of two elements longitudinal slot array antenna

Figure 1-#	Slot-1 Length (mm)	Slot-2 Length (mm)	Slot width (mm)	Spacing between Slot-1 and Slot-2 (centre to centre) (mm)	Left plate to Slot-1 centre distance (mm)	Right plate to Slot-2 centre distance (mm)	Slot-1 Offset Waveguide Centre to slot Centre (mm)	Slot-2 Offset Waveguide Centre to slot Centre (mm)	Waveguide Length Left to right (mm)
(a)	16	16	1	19.8	9.9	9.9	-3.5	+3.5	39.75
(b)	16	16	1	19.8	9.9	9.9	-3.5	-3.5	39.75
(c)	19.5	13.5	1	19.8	9.9	9.9	-3.5	+3.5	39.75
(d)	19.5	13.5	1	19.8	9.9	9.9	-3.5	-3.5	39.75
(e)	18	18	2	0	9.9	9.9	-8.5	+8.5	19.8
(f)	18	18	2	0	9.9	9.9	-8.5	+8.5	19.8
(g)	18.5	12.5	2	0	9.9	9.9	-8.5	+8.5	19.8
(h)	18.5	12.5	2	0	9.9	9.9	-8.5	+8.5	19.8

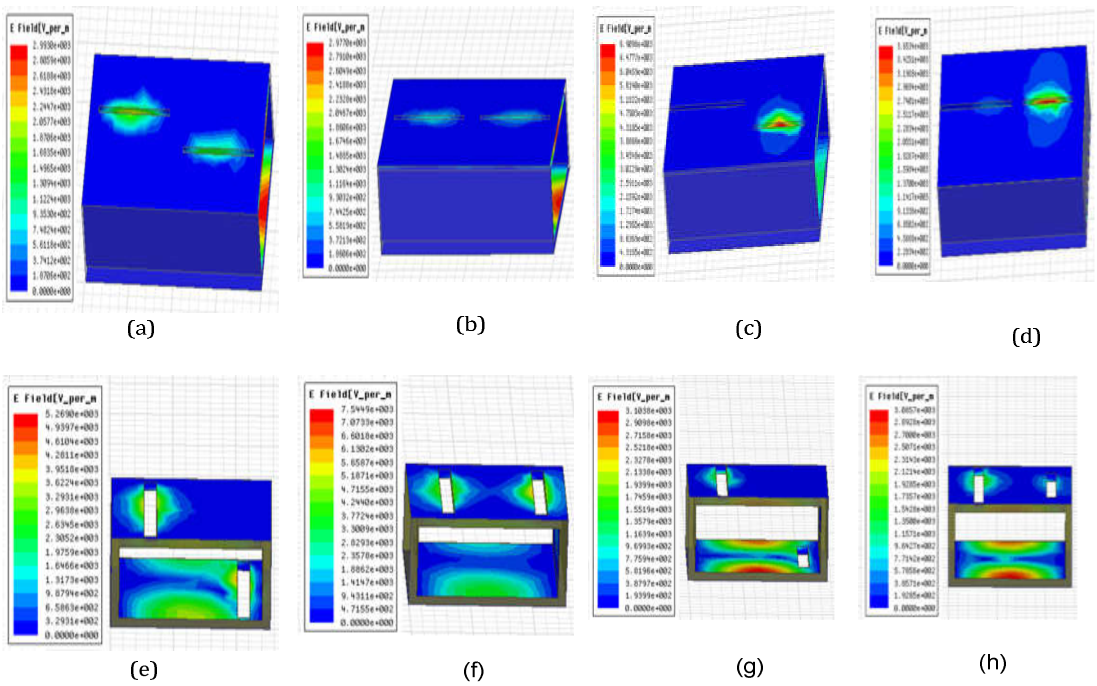

Fig. 2. Three dimensional view of simulated electric field (a) case-I (b) case-II, (c) case-III (d) case-IV, (e) case-V, (f) case-VI, (g) case-VII, and (h) case-VIII.

B. *Problem Formulation*

The following is a theoretical computation of the Transmission coefficient (T) and Reflection coefficient (Γ) using the Multiple Cavity Modeling Technique (MCMT).
The fields present at various locations for the two-element slot array antenna can be written as follows [10]:

Region 1: Waveguide

$$H_z^{inc} - \sum_{i=1,3} H_z^{wvg}(M_z^i) \tag{1}$$

Region n: cavity n

$$H_z^{cav}(M_z^{2n-1}) + H_z^{cav}(-M_z^{2n}) \quad n = 1, 2 \tag{2}$$

Region 3: Half space

$$\sum_{i=2,4} H_z^{ext}(M_z^i) \tag{3}$$

Four boundary conditions for each of the four apertures can be obtained by equating the tangential components of the magnetic field across different areas. Case I, Case II, Case III, Case IV, Case V, Case VI, Case VII, and Case VIII are the eight different circumstances for which this can be done. Four boundary conditions for each of the four apertures can be obtained by equating the tangential components of the magnetic field across different areas. Eight different scenarios—case I, case II, case III, case IV, case V, case VI, case VII, and case VIII—can be handled in this way. The electric field distribution across different apertures under the given boundary conditions can be found by using Glarkins' specialisation method of moments [9]. Equations (4) and (5) make it easy to obtain different scattering parameters once the electric field apertures have been established [11, 12]. Here, "2Li" stands for the ith slot's length, "2a" for the guide width, "2t" for the slot/waveguide wall thickness, and "2b" for the guide height. "2Wi" represents the slot width, while "xi" represents the offset of the ith slot. Along with the electric field connected to the ith slot, "k" is the wave number and "$\gamma_{m,n}$" is the propagation constant, specifically for TEm,n.

$$S(p) = \frac{p\pi}{(2L_i\gamma_{mn})}.$$

$$\Gamma = \frac{\pi^2 W_i}{4a^3 b\,\eta\kappa\beta^2} \times \left[\sin\left(\frac{\pi x_i}{2a}\right) \sin c\left(\frac{\pi W_i}{2a}\right) \sum_{p=1}^{M} \frac{S(p)}{1+S^2(p)} \begin{bmatrix} j\sinh(\beta L_i) if\ p\ even \\ \cosh(\beta L_i) if\ p\ odd \end{bmatrix} \right] \tag{4}$$

$$T = 1 + \frac{\pi^2 W_i}{4a^3 b\,\eta\kappa\beta^2} \times \left[\sin\left(\frac{\pi x_i}{2a}\right) \sin c\left(\frac{\pi W_i}{2a}\right) \sum_{p=1}^{M} \frac{S(p)}{1+S^2(p)} \begin{bmatrix} j\sinh(\beta L_i) if\ p\ even \\ \cosh(\beta L_i) if\ p\ odd \end{bmatrix} \right] \tag{5}$$

II. RESULSTS

The Scattering parameters like as Transmission Coefficient (T or S_{21}) and Reflection Coefficient (Γ or S_{11}) for each of the eight design instances (instances I through VIII) were calculated using MATLAB algorithms based on the proposed model. These computations were based on the Multiple Cavity Modeling Technique (MCMT), which provides an effective semi-analytical method for predicting electromagnetic behavior. Ansoft HFSS was used to compare the full-wave simulation results with the MCMT-derived data for each scenario. Fig. 3 and 4, which span the whole X-band operating range from 8.2 GHz to 12.4 GHz, offer this comparative analysis. Across all design situations, the results demonstrate a high degree of agreement between the HFSS-simulated results and the theoretical values calculated using MCMT. For example, in Case III and Case VI, the resonance behaviour, frequency bandwidth, and peak transmission of the $|S_{11}|$ and $|S_{21}|$ values are in near alignment. The intrinsic variations in mesh discretization systems and numerical solvers between MATLAB-based MCMT models and HFSS are responsible for the little variations seen in a few frequency spots. This robust association demonstrates how well the MCMT model and its MATLAB implementation predict complex structures' electromagnetic responses. The concordance with HFSS results confirms that the MCMT approach is a quick and portable tool for preliminary design assessments.

S-parameters and gain response were used to assess the electromagnetic behavior of eight distinct structural cases (Case I–VIII) spanning the 8.2–12.4 GHz spectrum. The transmission coefficient ($|S_{21}|$), reflection coefficient ($|S_{11}|$), and total gain are shown in Figures 3 and 5, respectively.

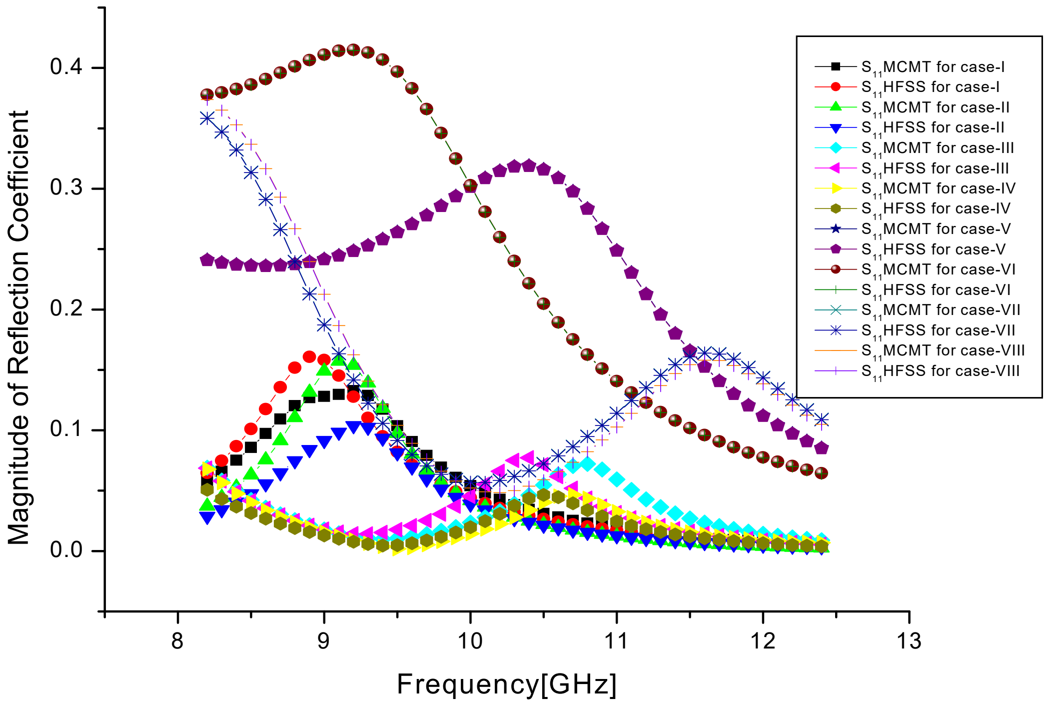

Fig. 3. Magnitude of reflection coefficient of eight different structural cases (from case-I to case-VIII).

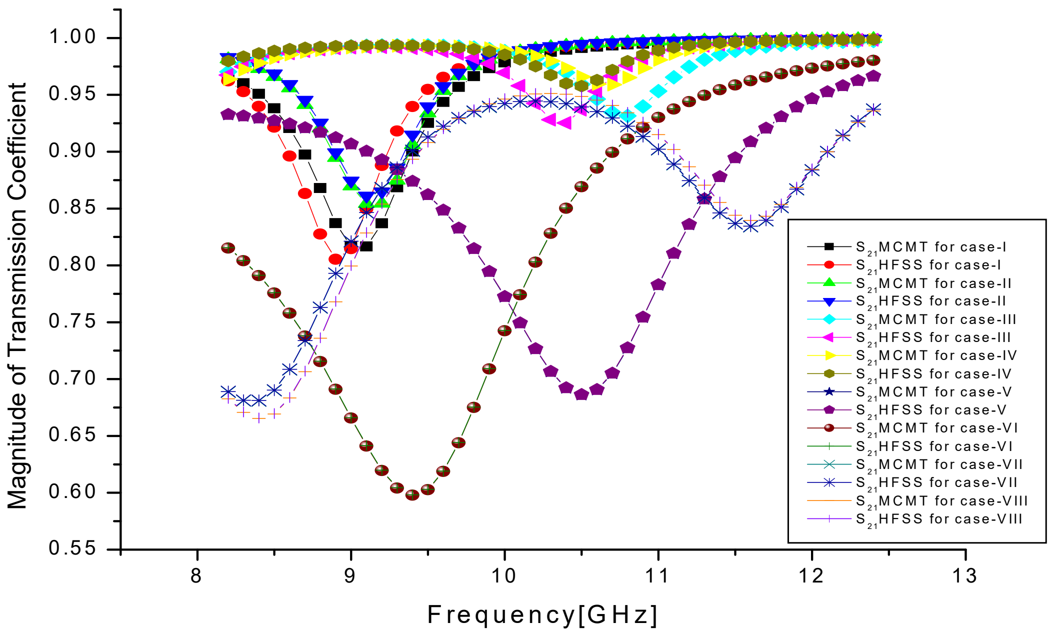

Fig. 4. Magnitude of transmission coefficient of eight different structural cases (from case-I to case-VIII).

III. DISCUSSION

A. Reflection Coefficient Design ($|S_{11}|$)

As shown in Fig. 3, the magnitude of the reflection coefficient across different cases demonstrates strong performance in Case III and case-VI, with values remaining below 0.15 (~–16.5 dB) for a wide range of frequencies. These cases exhibit broadband matching behavior, while case-V and case-IV reflect suboptimal performance with $|S_{11}|$ approaching or exceeding 0.3 in several regions.

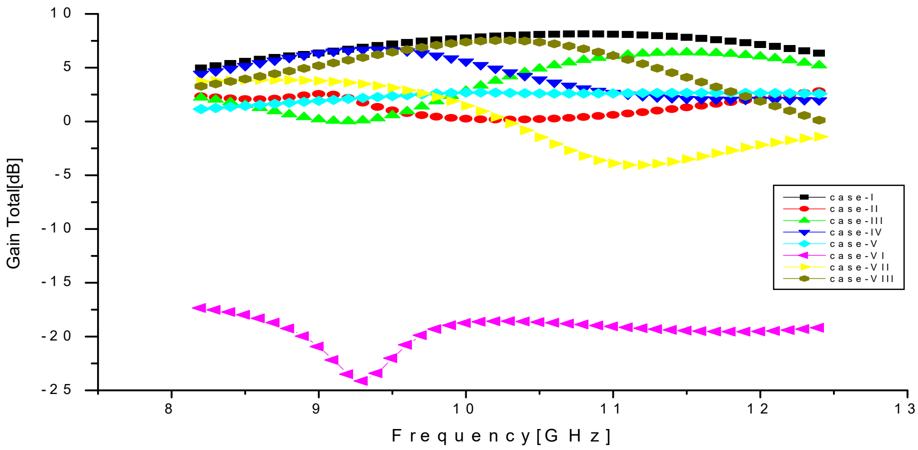

Fig. 5. The Gain of eight different structural cases (from case-I to case-VIII).

B. Transmission Coefficient ($|S_{21}|$)

In Figure 4, the transmission coefficient maintains high values (>0.9) across most of the frequency band for all designs, indicating efficient energy transfer. Case-VI and case-III again demonstrate superior characteristics, with $|S_{21}| > 0.95$ across most of the X-band. Conversely, Case V shows transmission dips below 0.75 between 9–11 GHz, indicating partial transmission losses due to mismatching or resonance interference.

C. Total Gain Analysis

Figure 5 provides the total gain profile across the same band. Case-I and case-VI stand out, offering consistently high gain (>6 dB), with case-I peaking near 9.5 dB. Case-IV shows significant degradation in gain performance, reaching as low as –24 dB, rendering it unsuitable for practical applications. The gain trends validate the electromagnetic compatibility of case-VI, aligning high gain with efficient matching and low reflection.

D. Overall performance Evaluation

From the comparative analysis:- case-VI is identified as the optimal design across all performance metrics: low reflection, high transmission, and robust gain.- case-III also performs admirably, especially in terms of impedance matching and forward transmission.- case-IV and case-V are less favorable due to low gain and inconsistent S-parameter behavior.

IV. CONCLUSION

This study examined the electromagnetic performance of eight different design configurations (from case-I to case-VIII) in the X-band frequency range (8.2–12.4 GHz) in terms of reflection coefficient, transmission coefficient, and total gain. To guarantee model fidelity and validation, the findings were achieved utilising both full-wave simulation via HFSS and the Multiple Cavity Modelling Technique (MCMT).

With broadband impedance matching ($|S_{11}|<0.15$), high transmission ($|S_{21}|>0.95$), and consistently good gain performance (>6 dB) over most of the frequency range, case-VI was the most optimal structure out of all the configurations. Though it had a little less gain, Case III likewise produced findings that were comparable, especially in terms of minimal reflection and effective signal propagation. On the other hand, case-IV had a very low gain (less than 20 dB), which made it unfit for practical use.

Excellent agreement across the majority of frequency bands and cases was confirmed by the comparison of MCMT and HFSS results; small differences were ascribed to meshing techniques and numerical accuracy. The efficiency of MCMT as a quick and computationally efficient substitute for initial electromagnetic analysis is demonstrated by this validation.

Overall, the study demonstrates that significant gains in bandwidth, radiation performance, and transmission efficiency can result from meticulous structural tweaking. The optimised, simulation-driven design of high-performance microwave components for X-band applications, including radar, satellite communication, and wireless sensing systems, is made possible by the validated modeling technique that combines MCMT and HFSS.

ACKNOWLEDGEMENT

The authors thank Medicaps University for their support of the study.

REFERENCES

[1]. T. V. Trinh, S Trinh Van, K. Y Lee, Y Yang, and K. C. Hwang, Design of a low-cost low-side lobe-level differential-fed SIW slot array antenna with zero beam squint. *Appl. Sci.* 12(21), pp. 1-12, 2022.

[2]. K.C. Gupta, R. Garg, I. Bahl, P. Bhartia, *"Microstrip Lines and Slotlines"*, Artech House, Norwood, MA, 1996.

[3]. D.M. Pozar, *"Microwave Engineering"*, 4th ed., Wiley, New York, 2011.

[4]. R. Garg, P. Bhartia, I. Bahl, A. Ittipiboon, *"Microstrip Antenna Design Handbook"*, Artech House, Boston, 2001.

[5]. K .L. Wong, *"Compact and Broadband Microstrip Antennas"*, Wiley, New York, 2002.

[6]. C. A. Balanis, *"Antenna Theory: Analysis and Design"*, 3rd ed., Wiley, New York, 2005.

[7]. G.C. Southworth, "Microwave Transmission," *Bell System Technical Journal*, vol. 15, pp. 284–309, 1936.

[8]. J. R. Wait, K.D. Stephan, "Slot antennas," *IEEE Transactions on Antennas and Propagation*, vol. 23, no. 3, pp. 417–420, 1975.

[9]. H. Booker, "Slot aerials and their relation to complementary wire aerials (Babinet's principle)," *Journal of the Institution of Electrical Engineers - Part IIIA: Radiolocation*, vol. 93, no. 4, pp. 620–626, 1946.

[10]. S. Silver, "*Microwave Antenna Theory and Design*", McGraw-Hill, New York, 1949.

[11]. Edelberg, A. Oliner, "Guided waves on periodically-loaded structures," *IRE Transactions on Microwave Theory and Techniques*, vol. 8, no. 6, pp. 706–718, 1960.

[12]. S. Das, A. Sanyal, "Mutual coupling between adjacent slots in a waveguide array," *IEEE Transactions on Antennas and Propagation,* vol. 19, no. 5, pp. 648–650, 1971.

[13]. R. S. Elliott, R. Stern, "Resonant length and offset for longitudinal slots in rectangular waveguides," *IEEE Transactions on Antennas and Propagation*, vol. 33, no. 10, pp. 1127–1129, 1985.

[14]. S. R. Rengarajan, "Analysis of tilted broadwall slots in rectangular waveguides," *IEEE Transactions on Antennas and Propagation,* vol. 38, no. 10, pp. 1577–1583, 1990.

[15]. Duan, Z. Shen, "Effect of surface distortion on performance of planar slotted waveguide arrays," *IEEE Transactions on Antennas and Propagation,* vol. 59, no. 6, pp. 2159–2165, 2011.

[16]. R. K Gayen, S. Das, "Broadband high-gain waveguide-fed slot array antennas using method of moments," *Progress in Electromagnetics Research C*, vol. 37, pp. 245–258, 2013.

[17]. Hare Ram Jha, Shiva Nand Singh, "Study of Scattering Parameters and Gain of two Longitudinal Slots of Same or Different Electrical Lengths Milled on a Single Waveguide for Series and Shunt Slot Array Antenna", *Proc. An International Conference on Microwave, Optical and Communication Engineering*, IIT Bhuvaneswar, India, pp. 280-283 December 18-20, 2015.

[18]. Hare Ram Jha, Shiva Nand Singh, "Study of Scattering Parameters and Gain of two longitudinal Slots of Same or Different Electrical Lengths Milled on either one or both Face of Broad Wall of a Waveguide for Shunt Slot Array Antenna*", Proc. A 3rd IEEE International Conference on Recent Advances in information*, ISM Dhanbad, March 3-5, 2016.

[19]. Hare Ram Jha, Shiva Nand Singh, "A New Design Approach for Tri-band Longitudinal Slot Doublet Array Waveguide Antenna as Applied to X-Band in Communication Systems", *International Journal of Microwave and Optical Technology*, Vol. 12, Issue. 1, pp. 30-36, 2017.